



HAL
open science

A cost driven predictive maintenance policy for structural airframe maintenance

Yiwei Wang, Christian Gogu, Nicolas Binaud, Christian Bes, Raphael T. Haftka,
Nam H. Kim

► **To cite this version:**

Yiwei Wang, Christian Gogu, Nicolas Binaud, Christian Bes, Raphael T. Haftka, et al.. A cost driven predictive maintenance policy for structural airframe maintenance. Chinese Journal of Aeronautics, 2017, 30 (3), pp.1242–1257. <10.1016/j.cja.2017.02.005>. <hal-01943031>

HAL Id: hal-01943031

<https://hal.science/hal-01943031v1>

Submitted on 29 May 2019

HAL is a multi-disciplinary open access archive for the deposit and dissemination of scientific research documents, whether they are published or not. The documents may come from teaching and research institutions in France or abroad, or from public or private research centers.

L'archive ouverte pluridisciplinaire **HAL**, est destinée au dépôt et à la diffusion de documents scientifiques de niveau recherche, publiés ou non, émanant des établissements d'enseignement et de recherche français ou étrangers, des laboratoires publics ou privés.



HAL Authorization



Chinese Society of Aeronautics and Astronautics
& Beihang University

Chinese Journal of Aeronautics

cja@buaa.edu.cn
www.sciencedirect.com



A cost driven predictive maintenance policy for structural airframe maintenance

Yiwei WANG^{a,*}, Christian GOGU^a, Nicolas BINAUD^a, Christian BES^a,
Raphael T. HAFTKA^b, Nam H. KIM^b

^a Université de Toulouse, INSA/UPS/ISAE/Mines Albi, ICA UMR CNRS 5312, Toulouse 31400, France

^b Department of Mechanical & Aerospace Engineering, University of Florida, Gainesville 32611, USA

Received 29 June 2016; revised 8 October 2016; accepted 12 December 2016

Available online 14 February 2017

KEYWORDS

Extended Kalman filter;
First-order perturbation
method;
Model-based prognostic;
Predictive maintenance;
Structural airframe
maintenance

Abstract Airframe maintenance is traditionally performed at scheduled maintenance stops. The decision to repair a fuselage panel is based on a fixed crack size threshold, which allows to ensure the aircraft safety until the next scheduled maintenance stop. With progress in sensor technology and data processing techniques, structural health monitoring (SHM) systems are increasingly being considered in the aviation industry. SHM systems track the aircraft health state continuously, leading to the possibility of planning maintenance based on an actual state of aircraft rather than on a fixed schedule. This paper builds upon a model-based prognostics framework that the authors developed in their previous work, which couples the Extended Kalman filter (EKF) with a first-order perturbation (FOP) method. By using the information given by this prognostics method, a novel cost driven predictive maintenance (CDPM) policy is proposed, which ensures the aircraft safety while minimizing the maintenance cost. The proposed policy is formally derived based on the trade-off between probabilities of occurrence of scheduled and unscheduled maintenance. A numerical case study simulating the maintenance process of an entire fleet of aircrafts is implemented. Under the condition of assuring the same safety level, the CDPM is compared in terms of cost with two other maintenance policies: scheduled maintenance and threshold based SHM maintenance. The comparison results show CDPM could lead to significant cost savings.

© 2017 Chinese Society of Aeronautics and Astronautics. Production and hosting by Elsevier Ltd. This is an open access article under the CC BY-NC-ND license (<http://creativecommons.org/licenses/by-nc-nd/4.0/>).

* Corresponding author.

E-mail addresses: yiwang@insa-toulouse.fr (Y. WANG), christian.gogu@univ-tlse3.fr (C. GOGU), nicolas.binaud@univ-tlse3.fr (N. BINAUD), christian.bes@univ-tlse3.fr (C. BES), haftka@ufl.edu (R.T. HAFTKA), nkim@ufl.edu (N.H. KIM).

Peer review under responsibility of Editorial Committee of CJA.



Production and hosting by Elsevier

1. Introduction

Fatigue damage is one of the major failure modes of airframe structures. Repeated pressurization/depressurization during take-off and landing cause many loading and unloading cycles which could lead to fatigue damage in the fuselage panels. The fuselage structure is designed to withstand small cracks, but if left unattended, the cracks will grow progressively and finally cause panel failure. It is important to inspect the aircraft reg-

ularly so that all cracks that have the risk of leading to panel fatigue failure should be repaired before the failure occurs.

Traditionally, the maintenance of aircraft is highly regulated through prescribing a fixed schedule. At the time of scheduled maintenance, the aircraft is sent to the maintenance hangar to undergo a series of maintenance activities including both engine and airframe maintenance. Structural airframe maintenance is a subset of airframe maintenance that focuses on detecting the cracks that can possibly threaten the safety of the aircraft. In this paper, maintenance refers to structural airframe maintenance while engine and non-structural airframe maintenance are not considered here. Structural airframe maintenance is often implemented by techniques such as non-destructive inspection (NDI), general visual inspection, detailed visual inspection (DVI), etc. Since the frequency of scheduled maintenance for commercial aircraft is designed for a low probability of failure, it is very likely that no safety threatening cracks exist during earlier life of majority of the aircraft. Even so, the intrusive inspection by NDI or DVI for all panels of all aircraft needs to be performed to guarantee the absence of critical cracks that could cause fatigue failure. Therefore, the inspection process itself is the major driver of maintenance cost.

Structural health monitoring (SHM) systems are increasingly being considered in aviation industry.¹⁻⁴ SHM employs a sensor network sealed inside the aircraft structures like fuselage, landing gears, bulkheads, etc., for monitoring the damage state of these structures. Once the health state of the structures can be monitored continuously or as frequently as needed, it is possible to plan the maintenance based on the actual or predicted information of damage state rather than on a fixed schedule. This spurs the research to predictive maintenance.

Prognostic is the prerequisite of the predictive maintenance. Prognostics methods can be generally grouped into two categories: data-driven and model-based. Data-driven approaches use information from previously collected data from the same or similar systems to identify the characteristics of the damage process and predict the future state of the current system. Data-driven prognosis is typically used in the cases where the system dynamic model is unknown or too complicated to derive. Readers can refer to^{5,6} that give an overview of data-driven approaches. Model-based prognostics methods assume that a dynamic model describing the behavior of the degradation process is available. For the problem discussed at hand, a model-based prognostics method is adopted since the fatigue damage models for metals have been well researched and are routinely used in the aviation industry for planning the structural maintenance.⁷⁻⁹

Predictive maintenance policies that aim to plan the maintenance activities taking into account the predicted information, or the “prognostics index” were proposed recently and attracted researcher’s attention in different domains.¹⁰⁻¹⁴ The most common prognostics index is remaining useful life (RUL).¹⁵⁻¹⁸ A large amount of methods on RUL estimation have been proposed such as filter methods (e.g., Bayesian filter,¹⁹ particle filter,^{20,21} stochastic filter,^{22,23} Kalman filter^{24,25}), and machine learning methods (e.g., classification methods,^{26,27} support vector regression²⁸). In addition to the numerical solutions for RUL prediction, Si et al.^{29,30} derived the analytical form of RUL probability density function. Some of the predictive maintenance policies adopting the RUL as a

prognostics index to dynamically update the maintenance time can be found in Refs.^{12, 14, 31}.

In some situations, especially when a fault or failure is catastrophic, inspection and maintenance are implemented regularly to avoid such failures by replacing or repairing the components that are in danger. In these cases, it would be more desirable to predict the probability that a component operates normally before some future time (e.g. next maintenance interval).³² Take the structural airframe maintenance as an example, the maintenance schedule is recommended by the manufacture in concertation with safety authorities. Arbitrarily triggering maintenance purely based on RUL prediction without considering the maintenance schedule might be disruptive to the traditional scheduled maintenance procedures due to less notification in advance. In addition, planning the structural airframe maintenance as much as possible at the scheduled maintenance stop when the engine and non-structural airframe maintenance are performed could lead to cost saving. To this end, instead of predicting the remaining useful life of fuselage panels, we consider the evolution of damage size distribution for a given time interval, before some future time (e.g. next maintenance interval). In other words, we adopt the “future system reliability” as the prognostics index to support the maintenance decision making. This distinguishes our paper from the majority existing work related to predictive maintenance.

The motivation developing advance maintenance strategies is to reduce the maintenance costs while maintaining safety. Researchers proposed many cost models to facilitate the comparison of maintenance strategies.^{10,12,13,33} All these cost analysis and comparison share one thing in common. The maintenance strategy is independent from unit cost (e.g., the set up cost, the corrective maintenance cost, the predictive maintenance cost, etc.) and the interaction between strategy and unit cost has not been considered, which in fact might affect the maintenance strategy in some situations. For example, in aircraft maintenance, it is beneficial to plan the structural airframe maintenance as much as possible at the same time of scheduled maintenance and only trigger unscheduled maintenance when needed. If the cost of unscheduled maintenance is much higher than the scheduled maintenance, the decision maker might prefer to repair as many panels as possible at scheduled maintenance to avoid unscheduled maintenance. That is to say the cost ratio of different maintenance modes could be a factor that affects the maintenance decision-making. In this paper, we take a step further from the existing work to take into account the effect of cost of different maintenance modes on the maintenance strategy, i.e., the cost ratio is taken as an input of maintenance the strategy and partially affects the decision-making. This is our motivation of developing the cost driven predictive maintenance (CDPM) policy for aircraft fuselage panel. By incorporating the information of predicted damage size distribution and the cost ratio between maintenance modes, an optimal panel repair policy is proposed, which selects at each scheduled maintenance stop a group of aircraft panels that should be repaired while fulfilling the mandatory safety requirement.

As for the process of prognosis, we consider four uncertainty sources. The item-to-item uncertainty accounts for the variability among the population, which is considered by using one degradation model to capture the common degradation

characteristics in the population, with several model parameters following initial distributions across the population to cover the item-to-item uncertainty. The epistemic uncertainty refers to the fact that for an individual degradation process the degradation model parameters are unknown due to lack of knowledge. This uncertainty can be reduced by measurements, i.e., the uncertainty of parameters can be narrow down with more measurements are available. The measurement uncertainty means that SHM data could be noisy due to harsh working conditions. The process uncertainty refers to the noise during the degradation process. This is considered through modeling the loading condition that affect the degradation rate as uncertain. To our best knowledge, these four uncertainties cover the most common uncertainties sources that are encountered during the prognostics procedure for fuselage panels.

To account for the uncertainties mentioned above, a state-space mode is constructed and the Extended Kalman filter (EKF) is used to incorporate the noisy measurements into the degradation model to give the estimates of damage size and model parameters as well as the estimate uncertainty (i.e., the covariance matrix between damage size and model parameters). After obtaining the estimates and its uncertainty from EKF, the straightforward way to predict the future damage size distribution is Monte Carlo method, which is time-consuming and gives only numerical approximation. Instead, we propose the first-order perturbation method to allow analytical quantification of the future damage size distribution.

As such, the main contributions of this paper are the following four aspects.

- Incorporating the “future system reliability” as a prognostics index to support the maintenance-decision making.
- Considering the cost ratio of different maintenance modes as the input the maintenance strategy.
- Taking into account four uncertainty sources: item-to-item uncertainty, epistemic uncertainty on the degradation model, measurement uncertainty and process uncertainty.
- Utilizing a first-order perturbation method to quantify the future damage distribution analytically.

The paper is organized as follows. Section 2 introduces the crack growth model used for modeling the degradation of the fuselage panels, degradation which induces the requirements for maintenance. This degradation process is affected by various sources of uncertainty, which are also described in Section 2. In order to be able to set-up the proposed predictive maintenance strategy we need to be able to predict the crack growth in future time while accounting for the sources of uncertainty present. To achieve this we first identify the parameters governing the crack growth based on crack growth measurements on the fuselage panels up to the present time. To carry out this identification we use the EKF, which is summarized in Section 3. Note that due to the various sources of uncertainty we do not identify a deterministic value but a probability distribution. Once this probability distribution of the parameters governing the crack growth determined, we need to predict the possible evolution of the crack size in future flights, which is achieved by a first-order perturbation (FOP) method also described in Section 3. The FOP method allows to determine the distribution of the crack size at an arbitrary future flight time. Based on this information we propose a

new maintenance policy, described in Section 5, which minimizes the maintenance cost. Section 5 implements a numerical study to evaluate the performance of the proposed maintenance policy. Conclusions and suggestions for future work are presented in Section 6.

2. State-space method for modeling the degradation process

2.1. State-space model

State-space modeling assumes that a stochastic dynamic system evolves with time. The states of the stochastic system are hidden and cannot be observed. A set of measurable quantities that are related with the hidden system states are measured at successive time instants. Then we have the following state-space model:

$$x_k = f(x_{k-1}, \theta_{k-1}, w_{k-1}) \quad (1)$$

$$z_k = h(x_k, v_k) \quad (2)$$

where $f(\cdot)$ and $h(\cdot)$ are the state transition function and the measurement function respectively. x_k is the unobserved state at time k . θ is the parameter of the state equation f . z_k is the corresponding measurements that generally contains noise. w_k and v_k are the process noise and measurement noise, respectively. Although the parameter θ is stationary, subscript $k - 1$ is used because its information is updated with time. In the following Sections 2.2 and 2.3, we model the equation f and h for the specific application of fatigue crack growth.

2.2. Fatigue crack growth model

The fatigue damage in this paper refers to cracks in fuselage panels. The Paris model⁷ is used to describe the crack growth behavior, as given

$$\frac{da}{dk} = C(\Delta K)^m \quad (3)$$

where a is the crack size in meters. k is the time step, here the number of flight cycles. da/dk is the crack growth rate in meter/cycle. m and C are the Paris model parameters associated with material properties. ΔK is the range of stress intensity factor, which is given in Eq. (4) as a function of the pressure differential p , fuselage radius r and panel thickness t . The coefficient A in the expression of ΔK is a correction factor compensating for modeling the fuselage as a hollow cylinder without stringers and stiffeners.³³

$$\Delta K = A \frac{Pr}{t} \sqrt{\pi a} \quad (4)$$

By using Euler method, Eq. (3) can be rewritten in a discrete form and the discretization precision depends on the discrete step. Here the step is set to be one, which is the minimal possible value from the practical point of view, to reduce the discretization error. Then the discrete Paris model in a recursive form is given in Eq. (5)

$$a_k = a_{k-1} + C \left(A \frac{P_{k-1} r}{t} \sqrt{\pi a_{k-1}} \right)^m = g(a_{k-1}, P_{k-1}) \quad (5)$$

The pressure differential p can vary at every flight cycle around its nominal value \bar{p} and is expressed as

$$p_k = \bar{p} + \Delta p_k \quad (6)$$

in which Δp_k is the disturbance around \bar{p} and is modeled as a normal distribution random with zero mean and variance σ_p^2 . Since uncertainty in pressure is generally small, the first-order Taylor series expansion is used in this paper.³⁴ This gives:

$$a_k = g(a_{k-1}, \bar{p}) + \frac{\partial g(a_{k-1}, \bar{p})}{\partial p} \Delta p_{k-1} \quad (7)$$

where $\partial g(a_{k-1}, \bar{p})/\partial p$ is the first-order partial derivative of g with respect to p . Taking $(\partial g(a_{k-1}, \bar{p})/\partial p)\Delta p_{k-1}$ as the additive process noise and considering that \bar{p} is a given constant, Eq. (7) can be written as

$$a_k = f(a_{k-1}) + w_{k-1} \quad (8)$$

in which $f(a_{k-1}) = g(a_{k-1}, \bar{p})$ and

$$w_{k-1} = (\partial f(a_{k-1})/\partial p)\Delta p_{k-1} \quad (9)$$

According to Eq. (7) the additive process noise w_k follows a normal distribution with mean zero and variance Q_k , given in Eq. (10). Note that Q_k can be calculated analytically.

$$\begin{aligned} Q_k &= ((\partial f(a_k, \bar{p})/\partial p)\sigma_p)^2 \\ &= (Cm(Ar/t)^m(\bar{p})^{m-1}(\pi a_k)^{m/2}\sigma_p)^2 \end{aligned} \quad (10)$$

2.3. Measurement model

Due to harsh working conditions and sensor limitations, the monitoring is imperfect and generally contains noise. The measurement data is modeled as

$$z_k = a_k + v_k \quad (11)$$

Note that Eq. (11) is used to simulate the actual measurement data. Eqs. (8) and (11) are respectively the state transition function and the measurement function in the state-space model.

3. Prognostics method for individual panel

Prognostic is the prerequisite of the predictive maintenance. In this paper, the model-based prognostics method is applied, which is tackled with two sequential phases: (1) estimation of

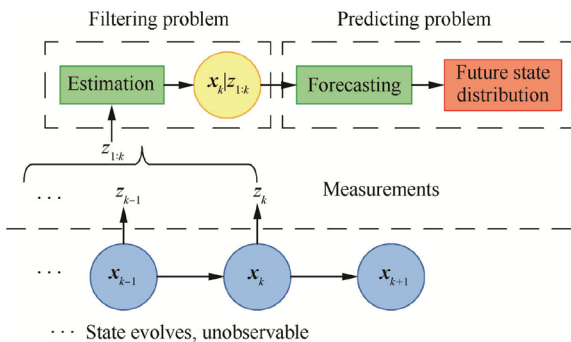


Fig. 1 Illustration of model-based prognostics.

fatigue crack size as well as the unknown model parameters, and (2) prediction of future crack size distribution. As illustrated in Fig. 1, the true system state is hidden and evolves over time. The measurements related to the state are obtained at a successive time step k . By using the measurements data up to the current time, the state and parameters of the state equation can be estimated. This process is also known as a filtering problem. Based on the estimated states and parameters, the state distribution in future time can be predicted. In this paper, the filtering problem is addressed by the EKF, and a proposed first-order perturbation method is used to predict the state distribution evolution in future times. In this section, the approaches for dealing with the two phases of model-based prognostics are presented respectively in Sections 3.1 and 3.2 briefly, since the main focus of this paper is the maintenance policy. The interested reader could refer to Ref.⁵ for more details on this approach.

3.1. State-parameter estimation using EKF

EKF is used to filter measurement noise based on a given state-space model. EKF thus allows to estimate a smooth variation of the state variable (crack size in our case) as well as the state-parameters (m and C in our case) governing these variations.

When performing state-parameter estimation using the EKF, the parameter vector of interest is appended onto the true state to form a single augmented state vector. The state and the parameters are estimated simultaneously. In Paris' model, m and C are the unknown parameters that need to be estimated. Therefore, a two-dimensional parameter vector is defined as

$$\theta = [m, C]^T \quad (12)$$

Appending θ to the state variable, that is crack size a , the augmented state vector is defined in Eq. (13), where the subscript "au" denotes the augmented variables.

$$\mathbf{x}_{\text{au}} = [a, m, C]^T \quad (13)$$

Then the state transition function and the measurement function in Eqs. (8) and (11) can be extended in a state-space model form as illustrated in Eq. (14). In this way, the estimation for Paris' model parameters and crack size is formalized as a nonlinear filtering problem. EKF is applied on the extended system in Eq. (14) to estimate the augmented state vector at time k , i.e., $\mathbf{x}_{\text{au},k} = [a_k, m_k, C_k]^T$. The EKF is used as a black box in the present work and the detail of the algorithm will not be presented here. Interested readers are referred to Ref.³⁵ for a general introduction to EKF and to Ref.²⁴ for its implementation to state-parameter estimation in Paris' model. By applying EKF, at each flight cycle, the posterior estimation of the augmented state vector, i.e., $\hat{\mathbf{x}}_{\text{au},k} = [\hat{a}_k, \hat{m}_k, \hat{C}_k]^T$, and the corresponding covariance matrix \mathbf{P}_k , characterizing the uncertainty in the estimated parameters, are obtained.

$$\begin{cases} \begin{bmatrix} a_k \\ m_k \\ C_k \end{bmatrix} = \begin{bmatrix} f(a_{k-1}) \\ m_{k-1} \\ C_{k-1} \end{bmatrix} + \begin{bmatrix} w_{k-1} \\ 0 \\ 0 \end{bmatrix} \\ z_k = a_k + v_k \end{cases} \quad (14)$$

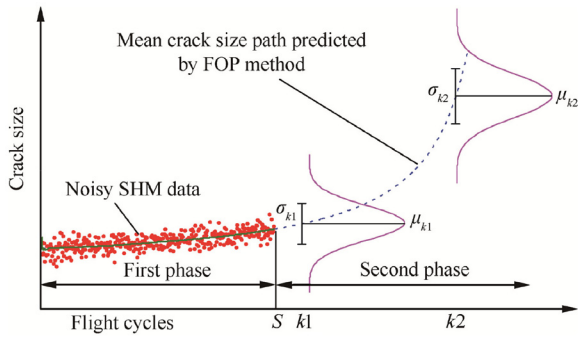


Fig. 2 Schematic diagram of model-based prognostics.

3.2. First-order perturbation (FOP) method for predicting the state distribution evolution

We propose the FOP method to address the second phase of model-based prognostics, i.e., the predicting problem, as shown in Fig. 1. For the context of crack growth, it allows to calculate analytically the crack size distribution at any future cycle. Fig. 2 illustrates the schematic diagram of the two phases of the discussed model-based prognostics method. The noisy measurements are collected up to the current cycle $k = S$. The EKF is used to filter the noise to give estimates for the crack size and the model parameters. At time S , the following information is given by the EKF and will be used as initial conditions of the second phase:

- expected value of the augmented state vector, $\hat{\mathbf{x}}_{\text{au},S} = [\hat{a}_S, \hat{m}_S, \hat{C}_S]^T$
- covariance matrix of the augmented state vector \mathbf{P}_S .

According to the EKF, the state vector $\mathbf{x}_{\text{au},S}$ follows a multivariate normal distributed with mean $\hat{\mathbf{x}}_{\text{au},S}$ and covariance \mathbf{P}_S , presented as

$$\mathbf{x}_{\text{au},S} \sim N(\hat{\mathbf{x}}_{\text{au},S}, \mathbf{P}_S) \quad (15)$$

Based on this information, in the second phase, the FOP is used to calculate analytically the mean and standard deviation, denoted by μ_k and σ_k , of the crack size distribution at any future cycle k starting from $S + 1$. The derivation of the FOP method is detailed in Appendix A. The dashed curve in the second phase represents the mean trajectory of the crack size estimated by the first-order perturbation method, i.e., $\{\mu_k | k = S + 1, S + 2, \dots\}$. For illustrative purpose, the crack size distribution at two arbitrary flight cycles $k1$ (based on μ_{k1} and σ_{k1}) and $k2$ (based on μ_{k2} and σ_{k2}) are given as examples.

It should be noted that the cost-driven predictive maintenance (CDPM) strategy to be presented in the following section considers an aircraft being composed of N_a panels. For each panel, the model-based prognostics process implemented by EKF-FOP method is applied. i.e., for each panel, we use EKF to estimate the Paris' model parameters and crack size from noisy measurements of the crack size at different flight cycles. Then we use the FOP method to predict the crack size distribution at a future time based on the information given by EKF (refer to Fig. 2). Once the crack size distribution at a future time is available for each panel, this prediction information is incorporated into the CDPM to help maintenance

decision-making. The details of CDPM strategy are presented next in Section 4.

4. Cost-driven predictive maintenance (CDPM) policy

Currently, aircraft maintenance is performed on a fixed schedule. Suppose that the aircraft undergoes the routine maintenance according to a schedule $T_n = T_1 + (n - 1)\delta T$, where $n = 1, 2, \dots$, is the number of scheduled maintenance stop, T_n denotes the cumulative flight cycles at the n th stop, T_1 is the number of flight cycles from the beginning of the aircraft lifetime to the first scheduled maintenance stop. δT is the interval between two consecutive scheduled maintenance stops after T_1 . Note that $T_1 > \delta T$ because fatigue cracks propagate slowly during the earlier stage of the aircraft lifetime. With usage and ageing, the aircraft needs maintenance more frequently. The schedule $\{T_n\}$ is determined by aircraft manufacturers in concertation with certification authorities and aims at guaranteeing the safety using a conservative scenario. For a given safety requirement this schedule may not be optimal, in terms of minimizing maintenance cost. Indeed a specific aircraft may differ from the fleet's conservative properties used in calculating the maintenance schedule and possibly require fewer maintenance stops.

By employing the SHM system, the damage state can be traced as frequently as needed (e.g. every 100 cycles) and the maintenance can be asked at any time according to the aircraft's health state rather than a fixed schedule. This causes an unscheduled maintenance that could happen anytime throughout the aircraft lifetime and generally occurs outside of the scheduled maintenances. Triggering a maintenance stop arbitrarily is significantly disturbing to the current scheduled maintenance practice due to no advance notification (e.g., less preparation of the maintenance team), unavailable tools, lack of spare parts, etc. These factors lead unscheduled maintenances to be more expensive. Therefore, we attempt as much as possible to plan the structural airframe maintenance at the time of the scheduled maintenance and avoid the unscheduled maintenance in order to reduce the cost.

On the other hand, it makes sense to skip some scheduled maintenance stops. Since the frequency of scheduled maintenance for commercial aircrafts is designed for a low probability of failure (10^{-7})³³, it is very likely that no large crack exists during earlier life of the majority of the aircraft in service. Thanks to the on-board SHM system, the damage assessment could be done in real time on site instead of in a hangar, leading to the possibility of skipping unnecessary scheduled maintenance if there are no life-threatening cracks on the aircraft. If a crack missed at schedule maintenance grows large enough to threaten the safety between two consecutive scheduled maintenances, an unscheduled maintenance is triggered at once. The frequent monitoring of the damage status would ensure the same level of reliability as scheduled maintenance. Recall that our objective is to re-plan the structural airframe maintenance while the engine and non-structural airframe maintenance are always performed at the time of scheduled maintenance.

In summary, it might be beneficial that in civil aviation industry to have the traditional scheduled maintenance work in tandem with the unscheduled maintenance. With this motivation, the CDPM policy is proposed whose overall idea is described below:

- The damage states of the fuselage panels are monitored continuously by the on-board SHM system and a damage assessment is performed every 100 flights (which approximately coincides with A-checks of the aircraft).
- At each assessment, as new arrived sensor data is available, the EKF is used to filter the measurement noise to provide the estimated crack size and parameters of crack growth model for each panel at current flight cycle.
- At the n th scheduled maintenance stop, before the aircraft goes into the maintenance hangar, for each panel, the crack propagation trajectory from maintenance stop n to $n + 1$ is predicted and the crack size distribution at next scheduled maintenance is obtained by using the first-order perturbation method. Taking into account this predicted information of each panel, the cost optimal policy decides to skip or trigger the current n th stop. If it is triggered, a group of specific panels is selected to be repaired based on the predicted information to minimize the expected maintenance cost. The algorithm of selecting a group of specific fuselage panels is called cost optimal policy and will be described in Section 4.5.
- During the interval of two consecutive scheduled maintenance stop, if there is a crack exceeding a safety threshold a_{maint} at damage assessment, an unscheduled maintenance is triggered immediately. The aircraft is sent to the hangar and this panel is repaired. The meaning and calculation of a_{maint} is discussed in Section 4.2.

4.1. Different behavior among individual panels of the population

Our objective is an aircraft with N_a fuselage panels. If all the manufactured panels are exactly the same and these panels work under exactly the same conditions and environment, then the panels will degrade identically. However, in practice, due to manufacturing and operation variability there is panel-to-panel variability.

In this study, the generic degradation model (Paris model) is used to capture the common degradation characteristics for a population of panels while the initial crack size a_0 and the degradation parameters m and C of each panel follows predefined prior distributions across the population to cover the panel-to-panel variability. When modeling one individual panel, a_0 , m and C are treated as “true unknown draws” from their prior distributions. By incorporating the sequentially arrived measurement data, the EKF is used for each panel to estimate the crack size and the material parameters and their distribution at time k . Here the superscript is the panel index and the subscript denotes the time instant.

In this paper, a_0 is assumed log normally distributed while m and $\log_{10}C$ are assumed to follow a multivariate normal distribution with a negative correlation coefficient.^{36–38}

4.2. Reliability of system level

The critical crack size that causes panel failure can be calculated by the empirical formula in Eq. (16), in which K_{IC} is a conservative estimate of the fracture toughness in loading Mode I and p_{cr} is also a conservative estimate of the pressure p given its distribution.

$$a_{\text{cr}} = \left(\frac{K_{\text{IC}}}{A \frac{p_{\text{cr}}}{i} \sqrt{\pi}} \right)^2 \quad (16)$$

Since the damage assessment is done every 100 cycles, if a crack size equals to a_{cr} is present in a panel in between two damage assessments, it will cause the panel failure at once. Therefore, another safety threshold a_{maint} , which is smaller than a_{cr} is determined to ensure safety between two damage assessments.

a_{maint} is calculated to maintain a 10^{-7} probability of failure of the aircraft between two damage assessments (100 cycles), i.e., when a crack size equals to a_{maint} is present on the fuselage panel, its probability of exceeding the critical crack size a_{cr} in next 100 cycles is less than 10^{-7} , hence ensure the safety of the aircraft until next damage assessment. At the time of damage assessment, once the maximal crack size among the panel population exceeds a_{maint} , the unscheduled maintenance is triggered immediately and the aircraft is sent to the hangar. Since this maintenance stop is unscheduled with very little advance notice only the panel having triggered the stop is replaced in order to minimize operational interruption.

4.3. Reliability of an individual panel

At the n th scheduled maintenance stop (the cumulative cycles is T_n) the crack size distribution of each individual panel before the next scheduled stop is predicted. For the i -th panel, the probability of triggering an unscheduled maintenance before next scheduled maintenance stops is denoted by $P(\text{us}|a^i)$. It is approximated by Eq. (17), i.e., the probability that the crack size of the i th panel at next scheduled maintenance $a_{T_{n+1}}^i$ is greater than a_{maint} , given the information provided by EKF at current scheduled maintenance stop, more specifically, the estimated crack size and material property parameters, $[\hat{a}_{T_n}^i, \hat{m}_{T_n}^i, \hat{C}_{T_n}^i]$, and the covariance matrix $\mathbf{P}_{T_n}^i$.

$$P(\text{us}|a^i) = \Pr(a_{T_{n+1}}^i > a_{\text{maint}} | [\hat{a}_{T_n}^i, \hat{m}_{T_n}^i, \hat{C}_{T_n}^i], \mathbf{P}_{T_n}^i) \quad (17)$$

The evolution of the crack size distribution from T_n to T_{n+1} is predicted by the FOP method presented in Section 3.2. According to the FOP method, $a_{T_{n+1}}^i$ is normally distributed with parameters $\mu_{T_{n+1}}^i$ and $\sigma_{T_{n+1}}^i$, which are calculated analytically. Thus $P(\text{us}|a^i)$ is computed as

$$P(\text{us}|a^i) = \int_{a_{\text{maint}}}^{\infty} \Phi(a_{T_{n+1}}^i | \mu_{T_{n+1}}^i, \sigma_{T_{n+1}}^i) da_{T_{n+1}}^i \quad (18)$$

where Φ is the probability density function of the normal distribution with mean $\mu_{T_{n+1}}^i$ and standard deviation $\sigma_{T_{n+1}}^i$.

Note that the probability of triggering an unscheduled maintenance of a panel is not proportional with its current crack size, i.e., it is not necessarily true that panel with larger crack size is more likely to trigger an unscheduled maintenance. Due to the variability of crack growth rate among panels as well as the uncertainty presented in the crack propagation process, a larger crack size at n th stop may have a lower probability of exceeding a_{maint} before next scheduled stop, compared with a smaller crack size.

4.4. Cost model

Some concepts as well as their notations are given firstly before the cost structure is introduced.

- d_n^j The repair decision for the j -th panel at the n th scheduled maintenance stop. It is a binary value defined as. Here the index j is based on the resorted rule that will be introduced Section 4.5.

$$d_n^j = \begin{cases} 1 & \text{if panel } j \text{ is repaired} \\ 0 & \text{if panel } j \text{ is not repaired} \end{cases} \quad (19)$$

- \mathbf{d}_n the decision vector such that $\mathbf{d}_n = [d_n^1, d_n^2, \dots, d_n^{N_a}]$. N_a is the total number of fuselage panels in an aircraft.
- c_0 the set up cost of SHM-based scheduled maintenance, which is a fixed cost that occurs every time the scheduled maintenance is triggered. The set up cost is assigned only once even if more than one panel is replaced.
- c_0^{un} the unscheduled set up cost, which is a fixed cost that occurs when unscheduled maintenance is triggered. Due to less advance notification, $c_0^{\text{un}} > c_0$.
- τ – a variable used to indicate the binary nature of scheduled maintenance. $\tau = 1$ means that the scheduled maintenance is triggered and the set up cost is incurred while $\tau = 0$ means this scheduled maintenance is skipped thus no set up cost.
- c_s the fixed cost of repairing one panel.
- c_{us} the repair cost at unscheduled maintenance, also called unscheduled repair cost, which is composed of two items, the unscheduled set up cost c_0^{un} plus the per panel repair cost c_s .

The expected maintenance cost at the n -th scheduled maintenance stop, denoted by $C(\mathbf{d}_n)$, is modeled as the function of the repair decision of each panel, as given in Eq. (20). The first two terms in Eq. (20) represent the scheduled repair cost while the last term represents the unscheduled repair cost. Here we assume that the probability for a panel to have more than one unscheduled repair is negligible.

$$C(\mathbf{d}_n) = c_0\tau + c_s \left(\sum_{j=1}^{N_a} d_n^j \right) + c_{\text{us}} \left(\sum_{j=1}^{N_a} (1 - d_n^j) \mathbf{P}(\text{us}|a^j) \right) \quad (20)$$

4.5. Cost optimal policy

The objective is to find the optimal grouping of several panels to be repaired to minimize the cost when the aircraft is at n -th scheduled maintenance stop. The algorithm is under the following assumptions:

- The probability for a panel to have more than one unscheduled repair during the aircraft lifetime is negligible.
- The probability to have more than one unscheduled repair at the same cycle is negligible. This means that having more than one panel repaired during unscheduled maintenance do not reduce the average cost of each panel.

At the n -th scheduled maintenance, for each panel, the probability of triggering an unscheduled maintenance between stop n and $n + 1$ is calculated according to section 4.3. Sort and arrange them in descending order such that

$$\begin{aligned} \mathbf{P}(\text{us}|a^1) &> \mathbf{P}(\text{us}|a^2) > \dots > \mathbf{P}(\text{us}|a^{i-1}) > \mathbf{P}(\text{us}|a^i) \\ &> \mathbf{P}(\text{us}|a^{i+1}) \dots > \mathbf{P}(\text{us}|a^{N_a}) \end{aligned} \quad (21)$$

Eq. (21) implies that the panel that is more likely to trigger an unscheduled maintenance is arranged in more front places. The motivation is that we are more concerned about the panels with higher probability of having unscheduled repair since unscheduled maintenance is more costly. In the following parts, the panel index refers to the order in Eq. (21).

Two sets I and J are defined.

$$I = \{1 \leq j \leq N | c_s \leq c_{\text{us}} \mathbf{P}(\text{us}|a^j)\} \quad (22)$$

$$J = \{1 \leq l \leq N | c_0 + l c_s \leq c_{\text{us}} \sum_{j=1}^l \mathbf{P}(\text{us}|a^j)\} \quad (23)$$

For zero set up cost (i.e., $c_0 = 0$), the set I contains the elements j such that repairing the j -th panel at current scheduled maintenance cost less than repairing it at an unscheduled maintenance stop. For any value of the set up cost, set J includes the elements j such that repairing all these j panels at scheduled maintenance cost less than at unscheduled maintenance. B_I and b_J are defined as the maximal value and the minimal value of set I and J , respectively. Note that B_I and b_J are scalars.

$$B_I = \max\{1 \leq j \leq N | c_s \leq c_{\text{us}} \mathbf{P}(\text{us}|a^j)\} \quad (24)$$

$$b_J = \min\{1 \leq l \leq N | c_0 + l c_s \leq c_{\text{us}} \sum_{j=1}^l \mathbf{P}(\text{us}|a^j)\} \quad (25)$$

A simple example is given below to explain the set I and J as well as to illustrate the meaning of B_I and b_J intuitively. Suppose there are N_a fuselage panels in an aircraft and this aircraft is now at the n -th scheduled maintenance stop. The objective is to decide whether this aircraft should undergo maintenance or should skip the current maintenance by evaluating the health state for each fuselage panel. Firstly, for each panel, its probability of triggering an unscheduled maintenance before next scheduled maintenance is calculated according to the process described in Section 4.3. Then these N_a probabilities are sorted in descending order according to Eq. (21). Afterward, each probability is multiplied by c_{us} and is compared with c_s . Suppose that we found the following relations:

$$\begin{aligned} c_s &\leq c_{\text{us}} \mathbf{P}(\text{us}|a^1) \\ c_s &\leq c_{\text{us}} \mathbf{P}(\text{us}|a^2) \\ c_s &\leq c_{\text{us}} \mathbf{P}(\text{us}|a^3) \\ c_s &\leq c_{\text{us}} \mathbf{P}(\text{us}|a^4) \\ c_s &> c_{\text{us}} \mathbf{P}(\text{us}|a^5) \\ c_s &> c_{\text{us}} \mathbf{P}(\text{us}|a^6) \\ &\vdots \\ c_s &> c_{\text{us}} \mathbf{P}(\text{us}|a^{N_a}) \end{aligned}$$

The above case means that for the first 4 panels, the cost of repairing any of them at current scheduled maintenance is less than the cost of repairing it at unscheduled maintenance. From the 5th panel to the last panel, it is not economic to repair any of them at current n -th scheduled maintenance since their probability of triggering unscheduled maintenance is very low. In this case, the set $I = \{1, 2, 3, 4\}$ and $B_I = 4$.

The above example considers the situation of repairing one single panel. Now we consider the situation of repairing a group of panels. Suppose we group the first l panels and then compare the following two costs: (1) the cost of repairing these l panels at current scheduled maintenance, i.e., $c_0 + lc_s$, and (2) the expected cost of repairing the l panels at unscheduled maintenance, i.e., $c_{us} \sum_{j=1}^l P(\text{us}|a^j)$. Suppose we found the following relations:

$$\begin{aligned} c_0 + c_s &> c_{us}P(\text{us}|a^1) \\ c_0 + 2c_s &> c_{us}(P(\text{us}|a^1) + P(\text{us}|a^2)) \\ c_0 + 3c_s &\leq c_{us}(P(\text{us}|a^1) + P(\text{us}|a^2) + P(\text{us}|a^3)) \\ &\vdots \\ c_0 + N_a c_s &\leq c_{us} \sum_{j=1}^{N_a} P(\text{us}|a^j) \end{aligned}$$

In the above case, $J = \{3, 4, \dots, N_a\}$ and $b_J = 3$.

From Eqs. (22)–(25), the following properties can be deduced straightforward.

$$1 \leq b_J < B_I \leq N_a \quad (26)$$

$$c_s \leq c_{us}P(\text{us}|a^j), \quad \text{for } j = 1, 2, \dots, B_I \quad (27)$$

$$c_s > c_{us}P(\text{us}|a^j), \quad \text{for } j = B_I + 1, B_I + 2, \dots, N_a \quad (28)$$

$$c_0 + lc_s > c_{us} \sum_{j=1}^l P(\text{us}|a^j), \quad \text{for } j = 1, 2, \dots, b_J - 1 \quad (29)$$

$$c_0 + b_J c_s \leq c_{us} \sum_{j=1}^{B_J} P(\text{us}|a^j) \quad (30)$$

The proof for Eq. (26) is given in Appendix B and Eqs. (27)–(30) can be easily derived from the definitions given in Eqs. (22)–(25). Now we discuss the cost optimal policy at the n th scheduled maintenance stop.

If set I is empty and the set up cost is zero (i.e., $c_0 = 0$), it means that for any panel the expected unscheduled repair cost is smaller than the scheduled one. In this case, the optimal repair policy is not to repair any panel at current scheduled maintenance stop, i.e., $d_n^*(a^j) = 0$, for $j = 1, 2, \dots, N_a$. Note that d_n^* denotes the optimal repair decision for the j -th panel at the n -th scheduled maintenance stop.

If the set I is not empty and the set up cost is zero (i.e., $c_0 = 0$), from Eqs. (27) and (28), it can be inferred that for any panel j that $j \leq B_I$ the expected unscheduled repair cost is larger than the scheduled one, while for any panel j that $j > B_I$, the expected unscheduled repair cost is smaller than the scheduled one. In the case of $I \neq \emptyset$, the set J could be either empty or non-empty. Now we discuss these two cases that $J = \emptyset$ and $J \neq \emptyset$, and derive the optimal repair decision in each cases.

If J is empty, it means that no matter how many panels are paired, the cost of repairing these panels at scheduled maintenance stop costs more than at unscheduled maintenance. Then the optimal maintenance policy is not to repair any panel at current scheduled maintenance stop, i.e., $d_n^*(a^j) = 0$, for $j = 1, 2, \dots, N_a$. Note that $I = \emptyset$ implies $J = \emptyset$ but we can have $J = \emptyset$ and $I \neq \emptyset$.

If J is not empty (i.e., $J \neq \emptyset$), from Eqs. (29) and (30), it can be known that for any panel j that $j < b_J$, repairing the j first panels at scheduled maintenance stop cost more than at unscheduled maintenance, and for $j = b_J$, repairing the j first panels at scheduled maintenance stop cost less than at unscheduled maintenance. As for $j > b_J$, repairing the j first panels at scheduled maintenance stop can be either better or worse. For example, we can have:

$$\begin{aligned} c_0 + c_s &> c_{us}P(\text{us}|a^1) \\ c_0 + 2c_s &\leq c_{us}(P(\text{us}|a^1) + P(\text{us}|a^2)) \\ c_0 + 3c_s &> c_{us}(P(\text{us}|a^1) + P(\text{us}|a^2) + P(\text{us}|a^3)) \quad \text{or} \\ c_0 + 3c_s &< c_{us}(P(\text{us}|a^1) + P(\text{us}|a^2) + P(\text{us}|a^3)) \end{aligned}$$

From Eq. (26), it can be known that the range $[1, N_a]$ are divided into three intervals by B_I and b_J , which are $[1, b_J]$, $[b_J + 1, B_I]$ and $[B_I + 1, N_a]$. To determine the optimal policy, it is clear that the b_J -first panels have to be repaired at the current scheduled maintenance (see Eq. (30)). In addition, since the expected unscheduled maintenance cost of panels in the interval $[b_J + 1, B_I]$ are larger than scheduled maintenance cost (see Eq. (27)), they should also be repaired at current scheduled maintenance stop. Finally, the optimal repair policy at n -th scheduled maintenance can be summarized as follows:

$$\begin{aligned} \text{If } J &= \emptyset \\ d_n^* &= 0, \quad \text{for } j = 1, 2, \dots, N \\ \text{Else} & \\ d_n^* &= \begin{cases} 1 & \text{for } j = 1, 2, \dots, B_I \\ 0 & \text{for } j = B_I + 1, B_I + 2, \dots, N_a \end{cases} \end{aligned} \quad (31)$$

The above decision implies that when J is empty, the optimal decision is not to repair any panel at the n -th scheduled maintenance stop. The expected cost under this situation is

$$C(d_n^*) = c_{us} \left(\sum_{j=1}^{N_a} P(\text{us}|a^j) \right) \quad (32)$$

When J is not empty, the optimal decision is to repair the first B_I panels and leave unattended the remaining ones. Accordingly, the cost in this case is

$$C(d_n^*) = c_0 + c_s B_I + c_{us} \left(\sum_{j=B_I+1}^{N_a} P(\text{us}|a^j) \right) \quad (33)$$

Then the optimized total maintenance cost during the aircraft lifetime, denoted as $C(d^*)$, is the sum of the cost at each scheduled maintenance $C(d_n^*)$.

$$C(d^*) = \sum_n C(d_n^*) \quad (34)$$

The rigorous mathematical proof regarding $C(d_n^*) < C(d_n)$, i.e., why d_n^* is the optimal decision is given in Appendix B. The cost optimal policy is integrated into the predictive policy, whose flowchart is illustrated in Fig. 3. The above repair deci-

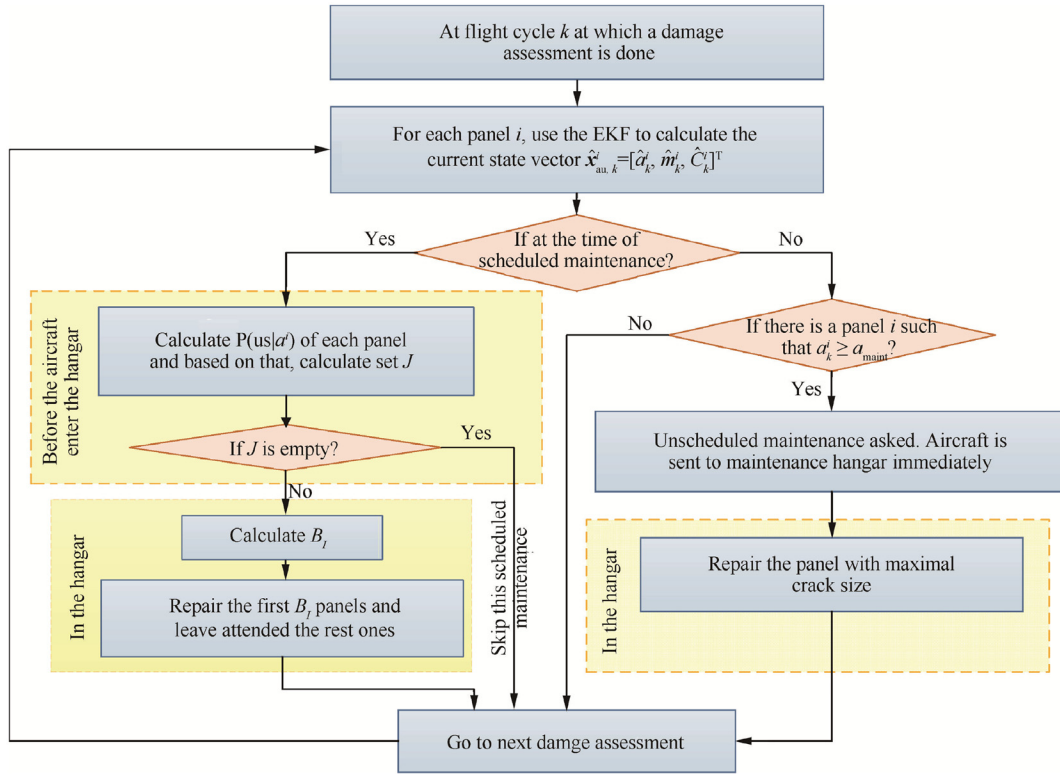


Fig. 3 Flow chart of CDPM.

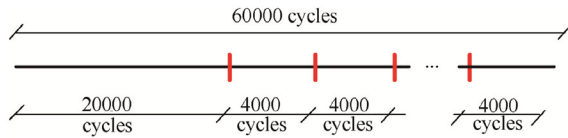


Fig. 4 Schedule of the scheduled maintenance process. Cycles represent the number of flights.

sion is made at each scheduled maintenance stop until the end aircraft's life. Then the total maintenance cost during aircraft lifetime $C(\mathbf{d}^*)$ can be calculated.

5. Numerical experiments

A fleet of $M = 100$ aircraft in an airline with each aircraft containing $N_a = 500$ fuselage panels is simulated. The potential application objective is a short range commercial aircraft with a typical lifetime of 60000 flight cycles. Traditionally, the maintenance schedule for this type of aircraft is designed such that the first maintenance is performed after 20000 flight cycles and the subsequent maintenance is every 4000 cycles until its end of life, adding up to 10 scheduled maintenances throughout its lifetime, as shown in Fig. 4.

To show the benefits of the CDPM, two other maintenance policies are compared with it. The first one is traditional scheduled maintenance and the second is a threshold-based SHM maintenance.

In traditional scheduled maintenance, at each maintenance stop, the aircraft is sent to the hangar to undergo a series of

inspections and all panels with a crack size greater than a threshold a_{rep} are repaired. The repair threshold a_{rep} is calculated to maintain the same reliability as CDPM between two consecutive scheduled maintenance stops over the entire fleet. Note that since this strategy seeks to guarantee the same reliability over the entire fleet it is more conservative than CDPM, which only has to guarantee the reliability for a single aircraft.

In threshold-based maintenance, the SHM is assumed to be used and the damage assessment is performed every 100 flights. The aim is the same as CDPM to skip some unnecessary early scheduled maintenance while guarantee the safety by triggering unscheduled maintenance. Specifically, at each scheduled maintenance stop, if there is no crack size exceeding a threshold $a_{\text{th-skip}}$, then the current scheduled maintenance is skipped. Between two consecutive scheduled maintenance stops, if a crack grows beyond a_{maint} , the unscheduled maintenance is triggered and all panels whose crack size is greater than a_{rep} are repaired. The flowchart of threshold-based maintenance is given in Fig. 5. For additional details on this threshold based maintenance strategy applied to fuselage panels, the reader could refer to Ref.³³.

Three design parameters characterize the threshold-based maintenance. First a_{maint} ensures the safety. It is defined and calculated the same as in CDPM, i.e., to maintain a 10^{-7} probability of failure between two damage assessments (every 100 cycles) for a given aircraft. Second $a_{\text{th-skip}}$ is calculated such that the probability of one crack exceeding a_{maint} before next scheduled maintenance is less than 5%. Finally, the repair threshold a_{rep} is set the same value as in traditional maintenance.

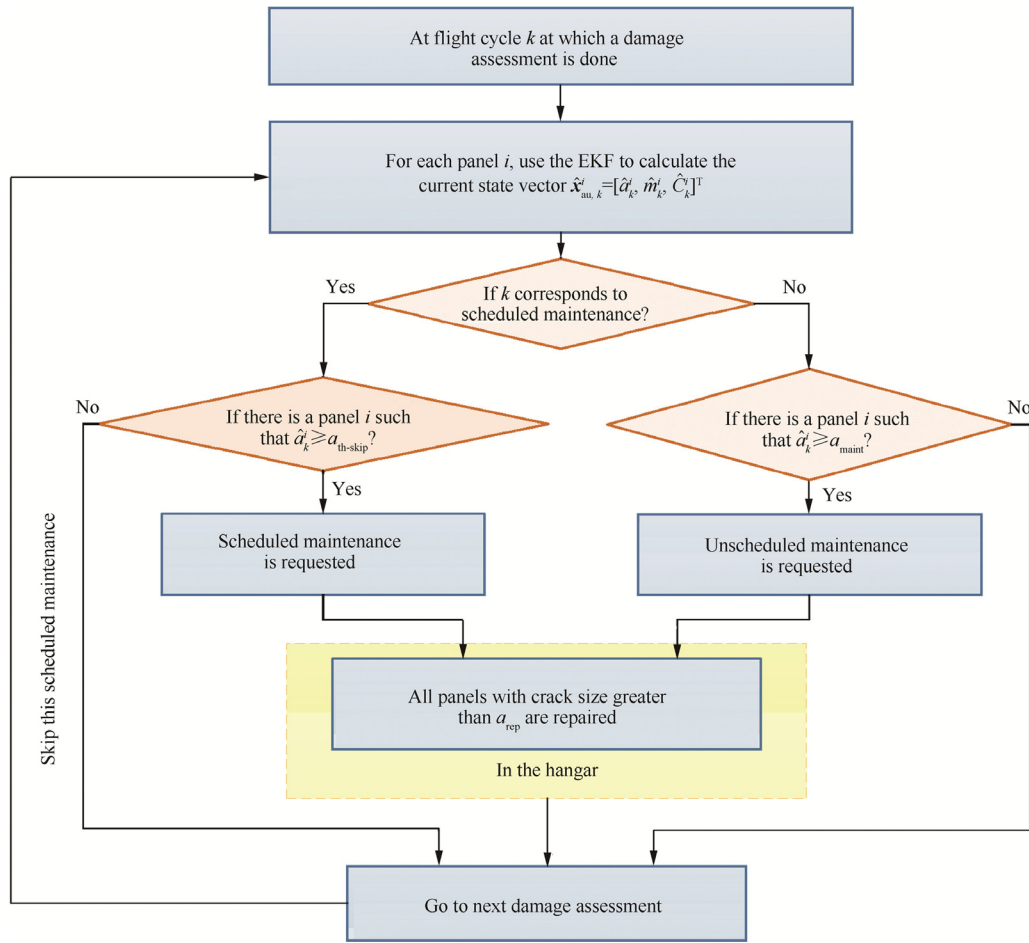


Fig. 5 Flow chart of threshold-based maintenance.

Table 1 Numerical values of geometry parameters.

Description	Notation	Value
Fuselage radius/m	r	1.95
Panel thickness/m	t	2×10^{-3}
Correction factor	A	1.25

Note the difference between threshold-based maintenance and the CDPM. In CDPM, the decision of whether or not to repair a panel is treated individually for each panel depending on the relation between the cost ratio (c_s/c_{us}) and the probability of triggering unscheduled maintenance. While in the threshold-based maintenance, this decision depends on the fixed threshold a_{rep} , which is determined for the entire fleet.

5.1. Input data

The values of the geometry parameters defining the fuselage used in the numerical application have been chosen from Ref.³³ and are reported in Table 1. These values are time-invariant. Recall that we define a correction factor A for stress intensity factor, which intends to account for the fact that the

Table 2 Numerical values of the uncertainties on a_0 , m , C and p .

Description	Notation	Type	Value
Initial crack size/ m	a_0	Lognormal	$\ln N(0.3 \times 10^{-3}, 0.0 \times 10^{-3})$
Paris model parameters	m, C	Multivariate	$N(\mu_m, \sigma_m, \mu_C, \sigma_C, \rho)$
Mean of m	μ_m		3.6
Mean of C	μ_C		$\lg(2 \times 10^{-10})$
C.C. ^a of m and C	ρ		-0.8
Standard deviation of m	σ_m		3%COV ^b
Standard deviation of C	σ_C		3%COV
Pressure/MPa	p	Normal	$N(0.06, 3\%COV)$

^a C.C. is correlation coefficient.

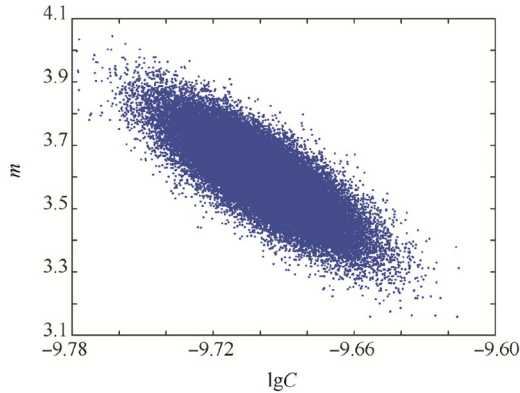
^b COV means coefficient of variation.

fuselage is modeled as a hollow cylinder without stringers and stiffeners.

As discussed in Section 4.1, we use the Paris model to capture the common degradation characteristics for a population of panels while the initial crack size a_0 and the Paris model

Table 3 Numerical values of thresholds.

Notation	Description	Value
a_{cr}	The critical crack size cause panel fail (m)	59.6×10^{-3}
a_{maint}	The safety threshold for triggering unscheduled maintenance (m)	47.4×10^{-3}
a_{rep}	The repair threshold (m)	4.3×10^{-3}
$a_{th-skip}$	The skip threshold used in threshold-based maintenance (m)	5.0×10^{-3}

**Fig. 6** Illustration of the population of m and C .

parameters m and C of each panel are drawn from prior distributions to model the panel-to-panel uncertainty. In addition, for each panel, during the crack propagation process, the pressure differential p varies from cycle to cycle and is modeled as a normal random variable. See Section 2.2 for details. The uncertainties for a_0 , m and C and p are given in Table 2. The numerical values of thresholds used are given in Table 3. At the beginning of the simulation, 500×100 samples of a_0 , m and C are drawn and assigned to each panel while p is drawn every cycle during the crack growth process. The 50,000 samples of m and C are illustrated in Fig. 6.

One thing needs to clarify. The uncertainties of a_0 , m and C given in Table 2 are the panel-to-panel uncertainty representing the variability among panels population. These 500×100 samples, denoted as $[a_0^i, m^i, C^i]^T$, ($i = 1, 2, \dots$), are assigned to each panel to form the initial condition of the i -th panel. Due to lack of knowledge on single panel, these samples are

regarded as “true unknown draws” that need to be estimated by the EKF. During the EKF process, for the i th panel, the initial guess for $[a_0^i, m^i, C^i]^T$ are randomly given and is fed to EKF as the start point. As the noisy measurements arrive sequentially, EKF incorporates the measurements and gives the optimal estimates to the crack size and model parameters at time k , denoted as $[\hat{a}_k^i, \hat{m}_k^i, \hat{C}_k^i]^T$. The estimation uncertainty reduces as time evolves due to more measurements are available. Due to limit space, the EKF process will not be detailed here. Readers could refer to Ref.²⁴.

Now we discuss the cost. The cost-related quantities are reported in Table 4. For the traditional scheduled maintenance, the set up cost is denoted as c_0^{tr} . For CDPM and the threshold-based maintenance, where the SHM system is used, the scheduled set up cost c_0 is only a fraction of c_0^{tr} due to the use of SHM system, leading to less labor intensive inspection compared to traditional inspection through DVI and NDI. This fraction is denoted as r_{shm} . In contrast, the unscheduled set up cost c_0^{un} is higher than c_0^{tr} due to less advance notice. A factor r_{un} is set to denote the higher set up cost incurred by unscheduled maintenance. Note that the per panel repair cost c_s is the same no matter in scheduled maintenance or unscheduled maintenance. It is the difference in set up cost that leads unscheduled maintenance to be costlier than scheduled maintenance.

At the n -th scheduled maintenance, the repair costs of traditional scheduled maintenance C_n^s , and that of threshold-based maintenance C_n^{thr} are given in the 8th and 9th rows of Table 4. The unscheduled repair cost of threshold-based maintenance c_{us}^{thr} and that of CDPM are given in the 10th and 11th rows. The symbol “ N_p ” in the last column of rows 8–10 denotes the number of panels repaired at that corresponding maintenance stop. Note that the unscheduled repair cost of CDPM c_{us} is composed of the unscheduled set up cost and the cost of repairing one panel since there is only one panel repaired once unscheduled maintenance is triggered.

Note that for traditional maintenance and the threshold-based maintenance, all cost-related quantities have no effect on the repair decision while in CDPM, the repair decision depends on the cost ratio c_s/c_{us} , thus relating to r_{un} . In the numerical experiments, c_0^{tr} and c_s are constants and are set to be 1.44 and 0.25 (Million \$) respectively. r_{shm} does not affect the repair decision, so it is assumed to be a constant value of 0.9 for simplicity. Different scenarios under varying r_{un} are studied. A series of discrete value, 0.9, 3, 5, 10, are chosen

Table 4 Cost-related quantities description.

Notation	In which maintenance policy it involves?	Description	How to calculate?
c_0^{tr}	Traditional scheduled maintenance	Set up cost/M\$	1.44
r_{shm}	Threshold-based maintenance and CDPM	Coefficient	0.9
r_{un}	Threshold-based maintenance and CDPM	Coefficient	0.9, 3, 5, 10
c_s	All three policies	Per panel repair cost/M\$	0.25
c_0	Threshold-based maintenance and CDPM	Scheduled set up cost/M\$	$c_0 = r_{shm}c_0^{tr}$
c_0^{un}	Threshold-based maintenance and CDPM	Unscheduled set up cost/M\$	$c_0^{un} = r_{un}c_0^{tr}$
C_n^s	Traditional scheduled maintenance	Scheduled repair cost at n th scheduled maintenance/M\$	$C_n^s = c_0^{tr} + c_s N_p$
C_n^{thr}	Threshold-based maintenance	Scheduled repair cost at n th scheduled maintenance/M\$	$C_n^{thr} = r_{shm}c_0^{tr} + c_s N_p$
c_{us}^{thr}	Threshold-based maintenance	Unscheduled repair cost/M\$	$c_{us}^{thr} = r_{un}c_0^{tr} + c_s N_p$
c_{us}	CDPM	Unscheduled repair cost/M\$	$c_{us} = r_{un}c_0^{tr} + c_s$

Table 5 Comparison results of different maintenance policies.

Scenario	Cost ratio (c_s/c_{us})	Maintenance policy	Avg. No. of M.S. ^a /aircraft	Avg. No. of U.M.S. ^b /aircraft	Avg. No. of R.P. ^c /aircraft	Avg. M.C. ^d /aircraft
$r_{un} = 0.9$	0.16	Scheduled	10	-	14.2	17.9
		Threshold-based	3.6	0	14.2	8.2
		CDPM	2.9	0.36	7.3	5.7
$r_{un} = 3$	0.05	CDPM	3.0	0.02	7.4	5.8
$r_{un} = 5$	0.03	CDPM	3.1	0	7.5	5.9
$r_{un} = 10$	0.01	CDPM	3.1	0	7.5	5.9

^a M.S. is Maintenance Stop.

^b U.M.S. is Unscheduled Maintenance Stop.

^c R.P. is Repaired Panels.

^d M.C. is structural Maintenance Cost.

for r_{un} . $r_{un} = 0.9$ indicates the unscheduled set up cost is as cheap as scheduled CPDM set up cost. This is an extreme case.

5.2. Results and discussion

The comparison among the three maintenance strategies is reported in Table 5. The 4th-6th columns give the average number per aircraft of the total maintenance stops throughout the lifetime, the unscheduled maintenance stops and the total repaired panels throughout the lifetime. The cost ratio (c_s/c_{us}) is given in the 2nd column. For traditional scheduled maintenance and the threshold-based maintenance, the cost-related coefficient the cost ratio does not affect the repair decision. From the practical point of view, the higher this ratio is, the less unscheduled maintenance there should be. The number of unscheduled maintenance in the 5th column matches well with this anticipation. When the cost of unscheduled maintenance is much higher (say 5 times higher or more) than that of the scheduled maintenance, the unscheduled maintenance is avoided by CDPM.

The 7th column gives the average structural maintenance costs per aircraft of different maintenance policies. According to the simulation results, no unscheduled maintenance is found in threshold-based maintenance. This does not mean that there will never be any but it is a very rare event which we do not capture with our fleet size. Therefore, the varying r_{un} has no effect to the cost of threshold-based maintenance. It can be seen that the CDPM leads to a significant cost savings compared with both traditional maintenance and threshold-based maintenance. The savings could be attributed to two aspects. Firstly, compared with the traditional scheduled maintenance, the CDPM skipped some unnecessary maintenance stops, thus reduced the set up cost. Secondly, CDPM significantly reduces the conservativeness compared to scheduled maintenance and threshold-based maintenance. In an aircraft fleet, there are two contributions to conservativeness level, the inter-aircraft variability and the intra-aircraft variability. The first one refers to that the worst aircraft in the fleet may have a larger crack size much sooner than the average, and the second means that in one aircraft, the fuselage panels may have different crack size and crack propagation rate. It is obvious that the scheduled maintenance is the most conservative one since it needs a very conservative repair threshold to cover both variabilities. Due to the conservative repair threshold, all panels with a crack size greater than a_{rep} are repaired even if some of them

have a very low growth rate and are not likely to fail until the aircraft's end of life. The threshold-based maintenance addresses part of the conservativeness which stems from the inter-aircraft variability and the intra-aircraft variability related to different crack size, but it is not able to handle the intra-aircraft variability related to different crack growth rates. In contrast, CDPM addressed both the variabilities by doing prognosis for each panel individually. Combined with an estimation of the crack size and the material property parameters of each panel at current time, CDPM predicts its crack growth trajectory in a future period of time and makes the decision of whether or not replacing this panel based on this predicted behavior. A simple example can illustrate this. Suppose there are two panels, A1, A2, with the same crack size that are greater than the repair threshold at the moment. According to the threshold-based strategies, both of them are repaired. While by using prognosis-based strategies, such as the proposed CDPM, we may find that the crack in A1 grows slowly and can be safe in a future period of time. A1 will then not be repaired. Based on the predicted information of each panel, the number of repaired panels is optimized. This reduces the number of repaired panels at each maintenance stop.

Note that the difference in structural maintenance cost for different cost ratios is about 5%. This means that the optimal maintenance policy allows to squeeze out these last few percent in terms of cost gains based on the objective measure of the cost ratio, without having to tune any additional parameters. It is also important to note how the optimal cost driven policy is affected by the level of uncertainties. We found that the cost optimal policy is most sensitive to the parameters of the maintenance decision (cost ratio) when the panel-to-panel variability is low compared to the prediction uncertainty. This can be explained as following: there are two items when predicting the crack size distribution at each scheduled maintenance, the first is predicting the mean and the second one is predicting the standard deviation after some additional cycles. If the panel-to-panel variability is large compared to the prediction uncertainty, then it is mainly the predicted mean value of crack size that matters and if the panel-to-panel variability is small compared to the prediction uncertainty then both the mean and standard deviation matter. The cost optimal policy is thus less sensitive in a large panel-to-panel variability case than in a low one even though the potential cost gains over traditional or threshold based maintenance would be larger with large panel to panel variability. On the other hand in a low panel-to-panel

variability case, while the potential cost gains become smaller, the maintenance policy becomes much more sensitive to maintenance decision parameters (cost ratio) and using the cost optimal policy makes an increasingly significant difference. The cost optimal policy would be even more sensitive to the cost ratios in applications where the distribution of unscheduled events between two scheduled maintenances is more gradual. This would be for example the case when the variability in material properties would be smaller and the prediction uncertainty due to measurement noise would be larger. The optimality of the maintenance strategy also guarantees that the structural maintenance cost is minimal without having to tune any additional parameters in the maintenance strategy. In addition, it allows avoiding having to choose a quantile (for example 95%) of the predicted distribution after some additional cycles when determining which panels to replace.

The cost difference between the CDPM and the traditional scheduled maintenance helps make the decision concerning the implementation of an SHM system on aircraft. More specifically, if the cost incurred by installing and operating an SHM system is less than cost saved by using SHM, then it is worth to install it on aircraft.

6. Conclusions

A cost driven predictive maintenance policy (CDPM) that ensures safety is proposed for structural airframe maintenance. The SHM system is assumed to be employed to track the fatigue crack in the fuselage panel continuously and to trigger unscheduled maintenance according to the fuselage health state. The CDPM leverages the benefit from both the scheduled and unscheduled maintenance. On one hand, it skips some unnecessary scheduled maintenance stops. On the other hand, it guarantees the aircraft safety by querying the health state of the fuselage frequently and triggering unscheduled maintenance whenever needed. For each aircraft panel, a model-based prognostics method is developed to estimate the current crack size and to forecast the future reliability of the panel. The proposed maintenance policy is developed at aircraft level. Based on the predicted reliability of all panels, it selects a group of panels which are to be repaired at a scheduled maintenance stop so as to minimize the cost. The CDPM is applied to the example of a short range commercial aircraft. The simulation results are compared with the traditional scheduled maintenance and the threshold-based maintenance in terms of the average number of maintenance stops, the average number of repaired panels and the average cost per aircraft under same operational conditions. The results show a significant cost reduction achieved by employing the CDPM. By comparing the cost difference between the CDPM and the scheduled maintenance, one can make the decision concerning the implementation of the SHM system on aircraft. More specifically, if the cost incurred by installing and operating an SHM system is lower than the cost saved by employing SHM, then it is worth to install the SHM system on the aircraft. Furthermore the proposed approach allows to assure the cost optimality of the maintenance policy without having to tune any additional parameters. The cost optimality then allows to squeeze out the last few percent of cost savings from prediction based maintenance.

Acknowledgements

This study was supported by UT-INSA Program (2013) and the authors gratefully acknowledge the support of the China Scholarship Council (CSC).

Appendix A. Derivation of the FOP method

At the end of first phase S , the following information is considered available from EKF and will be used as initial conditions for the second phase.

- expected value of the augmented state vector, $\hat{\mathbf{x}}_{\text{au},S} = [\hat{a}_S, \hat{m}_S, \hat{C}_S]^T$.
- covariance matrix of augmented state vector \mathbf{P}_S .

According to the EKF, the state vector $\mathbf{x}_{\text{au},S}$ is multivariate normally distributed with mean $\hat{\mathbf{x}}_{\text{au},S}$ and covariance \mathbf{P}_S , presented as

$$\mathbf{x}_{\text{au},S} \sim N(\hat{\mathbf{x}}_{\text{au},S}, \mathbf{P}_S) \quad (\text{A1})$$

Let us define:

$$f_L(a, m, C, p) = C \left(A \frac{p^r}{t} \sqrt{\pi a} \right)^m \quad (\text{A2})$$

The Paris model then becomes

$$a_k = a_{k-1} + f_L(a_{k-1}, m, C, p_{k-1}) \quad (\text{A3})$$

Note that here the index k starts from $S + 1$ and increases until $S + H$, i.e., $k = S + 1, S + 2, \dots, S + H$. Here H is the time span in future horizon. For the problem discussed at hand, the ‘‘expected trajectory’’ (trajectory that is obtained when the random variables assume their expected values) of the crack size is the sequence $\{\bar{a}_k | k = S + 1, S + 2, \dots, S + H\}$ obtained as a solution of the following equation with zero process noise and with the expected value $\bar{a}_S, \bar{m}, \bar{C}$ and \bar{p} as the initial conditions. Note that we use the hat symbol ‘‘ $\hat{}$ ’’ to denote the expected value of a random variable.

$$\bar{a}_k = \bar{a}_{k-1} + f_L(\bar{a}_{k-1}, \bar{m}, \bar{C}, \bar{p}) \quad (\text{A4})$$

Due to the presence of random noise and uncertainties, a_k, m, C and p_k are considered random. Let the symbol ‘‘ Δ ’’ denotes the perturbation from the expected values, then the real a_k, m, C and p_k can be modeled as

$$a_k = \bar{a}_k + \Delta a_k \quad (\text{A5})$$

$$m = \bar{m} + \Delta m \quad (\text{A6})$$

$$C = \bar{C} + \Delta C \quad (\text{A7})$$

$$p_k = \bar{p} + \Delta p_k \quad (\text{A8})$$

Δp_k is an uncertainty related to the cabin pressure differential, which varies from one flight cycle to another. On the other hand, Δm and ΔC are uncertainties related to the material of each panel and thus do not vary with time evolves. Recall the known information available at $k = S$, which will be the initial condition in the following derivation.

$$[\bar{a}_S, \bar{m}, \bar{C}]^T = [\hat{a}_S, \hat{m}_S, \hat{C}_S]^T \quad (\text{A9})$$

$$[\Delta a_S, \Delta m, \Delta C]^T \sim N(\mathbf{0}_{3 \times 1}, \mathbf{P}_S) \quad (\text{A10})$$

Subtracting Eq. (A4) from Eq. (A3), the perturbation of a_k is represented as

$$\Delta a_k = \Delta a_{k-1} + f_L(a_{k-1}, m, C, p_{k-1}) - f_L(\bar{a}_{k-1}, \bar{m}, \bar{C}, \bar{p}) \quad (\text{A11})$$

Given that f_L is differentiable, the first order approximation is used. Let $\lambda_{k-1} = [\bar{a}_{k-1}, \bar{m}, \bar{C}, \bar{p}]$, which is a known vector, then Eq. (A11) becomes

$$\begin{aligned} \Delta a_k = & \Delta a_{k-1} + \frac{\partial f_L(\lambda_{k-1})}{\partial a} \Delta a_{k-1} + \frac{\partial f_L(\lambda_{k-1})}{\partial m} \Delta m \\ & + \frac{\partial f_L(\lambda_{k-1})}{\partial C} \Delta C + \frac{\partial f_L(\lambda_{k-1})}{\partial p} \Delta p_{k-1} \end{aligned} \quad (\text{A12})$$

To make Eq. (A12) simpler we make the following substitution:

$$L_{k-1} = 1 + \frac{\partial f_L(\lambda_{k-1})}{\partial a} \quad (\text{A13})$$

$$M_{k-1} = \frac{\partial f_L(\lambda_{k-1})}{\partial m} \quad (\text{A14})$$

$$N_{k-1} = \frac{\partial f_L(\lambda_{k-1})}{\partial C} \quad (\text{A15})$$

$$w_{k-1}^L = \frac{\partial f_L(\lambda_{k-1})}{\partial p} \Delta p_{k-1} \quad (\text{A16})$$

in which w_{k-1}^L is the process noise, a normal variable with mean zeros and standard deviation σ_{k-1} , calculated by Eq. (A17). w_i^L and w_j^L ($i \neq j$) are considered independent.

$$\sigma_{k-1} = \frac{\partial f(\lambda_{k-1})}{\partial p} \sigma_p \quad (\text{A17})$$

Then Eq. (A12) becomes

$$\Delta a_k = L_{k-1} \Delta a_{k-1} + M_{k-1} \Delta m + N_{k-1} \Delta C + w_{k-1}^L \quad (\text{A18})$$

Eq. (A18) enables to calculate the perturbation of crack size at any cycle. Recalling Eq. (A10), the distribution of Δa_k can be analytically calculated as the function of the distribution of $[\Delta a_S, \Delta m, \Delta C]$. After k times iteration the analytical formula of calculating Δa_k is given in Eq. (A19). For simplicity, we use A_k , B_k and D_k represent the coefficient of Δa_S , Δm and ΔC respectively while E_k denotes the noise term.

$$\Delta a_k = A_k \Delta a_S + B_k \Delta m + D_k \Delta C + E_k \quad (\text{A19})$$

Note that in Eq. (A19), Δa_S , Δm and ΔC are stationary variables whose statistical distributions are time invariant. A_k , B_k and D_k are deterministic and evolve with time, which are calculated recursively with their initial values L_S , M_S , N_S , as shown in Eqs. (A20)–(A22). E_k is the only random variable whose distribution varies from cycle to cycle and is derived recursively by Eq. (A23). E_k is a linear combination of independent and identically distributed variables, it is a normal variable such that $E_k \sim N(0, F_k)$, in which F_k represents the variance of E_k . Using the recurrence of Eq. (A24), F_k can be obtained recursively with its initial value σ_s , given by Eq. (A17) Note that w_k^L and σ_k in Eqs. (A23) and (A24) refer to Eqs. (A16) and (A17), respectively.

$$A_k = L_k A_{k-1} \quad (\text{A20})$$

$$B_k = L_k B_{k-1} + M_k \quad (\text{A21})$$

$$D_k = L_k D_{k-1} + N_k \quad (\text{A22})$$

$$E_k = L_k E_{k-1} + w_k^L \quad (\text{A23})$$

$$F_k = L_k^2 F_{k-1} + \sigma_k^2 \quad (\text{A24})$$

Given that A_k , B_k , D_k are deterministic, and Δa_S , Δm , ΔC and E_k are random variables, Eq. (A19) can be rewritten as matrix form as $\Delta a_k = \mathbf{B}_k \boldsymbol{\beta}_k$, in which $\mathbf{B}_k = [A_k, B_k, D_k, 1]$ and $\boldsymbol{\beta}_k = [\Delta a_S, \Delta m, \Delta C, E_k]^T$.

Given $[\Delta a_S, \Delta m, \Delta C]^T \sim N(\mathbf{0}_{3 \times 1}, \mathbf{P}_S)$ and $E_k \sim N(0, F_k)$, $\boldsymbol{\beta}_k$ is a multivariate normal vector such that $\boldsymbol{\beta}_k \sim N(\boldsymbol{\mu}, \boldsymbol{\Sigma})$, in which $\boldsymbol{\mu} = [\mathbf{0}_{4 \times 1}]$ and $\boldsymbol{\Sigma} = \text{diag}(\mathbf{P}_S, F_k)$. Therefore, Δa_k is normally distributed with mean $\mathbf{B}_k \boldsymbol{\mu}$ and variance $\mathbf{B}_k \boldsymbol{\Sigma} \mathbf{B}_k^T$, which are calculated analytically.

$$\mathbf{B}_k \boldsymbol{\mu} = 0 \quad (\text{A25})$$

$$\mathbf{B}_k \boldsymbol{\Sigma} \mathbf{B}_k^T = [A_k, B_k, D_k] \mathbf{P}_S [A_k, B_k, D_k]^T + F_k \quad (\text{A26})$$

Given that $a_k = \bar{a}_k + \Delta a_k$ and \bar{a}_k is constant, a_k is a normal variable that $a_k \sim N(\mu_{ak}, \sigma_{ak})$, in which

$$\mu_{ak} = \bar{a}_k \quad (\text{A27})$$

$$\sigma_{ak} = \sqrt{\mathbf{B}_k \boldsymbol{\Sigma} \mathbf{B}_k^T} \quad (\text{A28})$$

The above formulas enable to compute analytically the evolution of the crack size distribution from cycle $S + 1$ to cycle $S + H$.

Appendix B. Proof of the cost optimal policy

In this Appendix, we give a mathematical proof of the cost optimal policy presented in Section 4.5. Eq. (26) in Section 4.5 is firstly proved as the prerequisites for the proof. Recall that in Eq. (26), it gives $1 \leq b_J < B_I \leq N_a$. Suppose the contrary

$$1 \leq B_I < b_J \leq N_a \quad (\text{B1})$$

Then we have

$$c_{us} \sum_{j=1}^{b_J} \mathbf{P}(\text{us}|a^j) = c_{us} \left(\sum_{j=1}^{B_I} \mathbf{P}(\text{us}|a^j) + \sum_{j=B_I+1}^{b_J} \mathbf{P}(\text{us}|a^j) \right) \quad (\text{B2})$$

Since $B_I < b_J$, according to Eq. (29) in Section 4.5, we have

$$c_{us} \left(\sum_{j=1}^{B_I} \mathbf{P}(\text{us}|a^j) \right) < c_0 + B_I c_s \quad (\text{B3})$$

And according to Eq. (27), we have

$$c_{us} \left(\sum_{j=B_I+1}^{b_J} \mathbf{P}(\text{us}|a^j) \right) < c_s (b_J - B_I) \quad (\text{B4})$$

Sum the inequalities Eqs. (B3) and (B4), we have

$$c_0 + B_I c_s > c_{us} \sum_{j=1}^{b_J} \mathbf{P}(\text{us}|a^j) \quad (\text{B5})$$

which is impossible since Eq. (30) in Section 4.5 is not satisfied. So $1 < b_J < B_I < N_a$.

Now, we prove the cost optimal repair policy. Reminder that the optimal policy \mathbf{d}_n^* is

If $J = \emptyset$

$$d_n^* = 0, \quad \text{for } j = 1, 2, \dots, N$$

Else

$$d_n^* = \begin{cases} 1 & \text{for } j = 1, 2, \dots, B_I \\ 0 & \text{for } j = B_I + 1, B_I + 2, \dots, N_a \end{cases}$$

The maintenance cost is a function of decision. Our objective is to prove $C(d_n) > C(d_n^*)$ for any maintenance policy d_n . Let us define the following set:

$$A = \{1 \leq j \leq B_I | d_n^j = 1\} \quad (\text{B6})$$

$$\bar{A} = \{1 \leq j \leq B_I | d_n^j = 0\} \quad (\text{B7})$$

$$B = \{B_I + 1 \leq j \leq N | d_n^j = 1\} \quad (\text{B8})$$

$$\bar{B} = \{B_I + 1 < j \leq N | d_n^j = 0\} \quad (\text{B9})$$

$|A|$, $|\bar{A}|$, $|B|$ and $|\bar{B}|$ are the cardinality of the set A , \bar{A} , B and \bar{B} , respectively. Obviously, we have the following: $|A| + |\bar{A}| = B_I$ and $|B| + |\bar{B}| = N_a - B_I$. The maintenance cost $C(d_n)$ is then computed as

$$C(d_n) = c_0 + c_s |A| + c_{us} \left(\sum_{j \in A} P(\text{us} | a^j) \right) + c_s |B| + c_{us} \sum_{j \in B} P(\text{us} | a^j) \quad (\text{B10})$$

Since $c_{us} P(\text{us} | a^j) \geq c_s$, for $j = 1, 2, \dots, B_I$ (refer to Eq. (27) in Section 4.5). Then we have $\sum_{j \in \bar{A}} c_{us} P(\text{us} | a^j) \geq c_s |\bar{A}|$, hence

$$\begin{aligned} & c_0 + c_s |A| + c_{us} \left(\sum_{j \in \bar{A}} P(\text{us} | a^j) \right) \\ & \geq c_0 + c_s |A| + c_s |\bar{A}| \\ & = c_0 + B_I c_s \end{aligned} \quad (\text{B11})$$

Since $c_{us} P(\text{us} | a^j) < c_s$, for $j = B_I + 1, B_I + 2, \dots, N_a$ (see Eq. (27)). Then we have

$$\begin{aligned} & c_s |B| + c_{us} \sum_{j \in B} P(\text{us} | a^j) \\ & > c_{us} \sum_{j \in B} P(\text{us} | a^j) + c_{us} \sum_{j \in \bar{B}} P(\text{us} | a^j) \\ & = \sum_{j=B_I+1}^{N_a} c_{us} P(\text{us} | a^j) \end{aligned} \quad (\text{B12})$$

Sum the inequalities Eqs. (B11) and (B12), then we have

$$\begin{aligned} & c_0 + c_s |A| + c_{us} \left(\sum_{j \in A} P(\text{us} | a^j) \right) + c_s |B| + c_{us} \sum_{j \in B} P(\text{us} | a^j) \\ & \geq c_0 + B_I c_s + \sum_{j=B_I+1}^{N_a} c_{us} P(\text{us} | a^j) \end{aligned} \quad (\text{B13})$$

The left term of the inequality is the maintenance cost $C(d_n)$ while the right term of the inequality is the optimal cost $C(d_n^*)$, so we have $C(d_n) > C(d_n^*)$. Up to now, the cost under any other decision d_n is greater than the cost under the optimal decision d_n^* has been proved.

References

- Zhao XL, Gao HD, Zhang GF, Ayhan B, Yan F, Kwan C, et al. Active health monitoring of an aircraft wing with embedded piezoelectric sensor/actuator network: I. Defect detection, localization and growth monitoring. *Smart Mater Struct* 2007;**65**:1208–17.
- Ignatovich SR, Menou A, Karuskevich MV, Maruschak PO. Fatigue damage and sensor development for aircraft structural health monitoring. *Theor Appl Fract Mech* 2013;**65**:23–7.
- Diamanti K, Soutis C. Structural health monitoring techniques for aircraft composite structures. *Prog Aerosp Sci* 2010;**46**(8):342–52.
- Ihn JB, Chang F. Detection and monitoring of hidden fatigue crack growth using a built-in piezoelectric sensor/actuator network: I. Diagnostics. *Smart Mater Struct* 2004;**13**(3):609.
- An D, Kim NH, Choi J-H. Practical options for selecting data-driven or physics-based prognostics algorithms with reviews. *Reliab Eng Syst Saf* 2015;**133**:223–36.
- Si X, Wang W, Hu C, Zhou D. Remaining useful life estimation – a review on the statistical data driven approaches. *Eur J Oper Res* 2011;**213**(1):1–14.
- Paris P, Erdogan F. A critical analysis of crack propagation laws. *J Basic Eng* 1963;**85**(4):528–33.
- Pugno N, Ciavarella M, Cornetti P, Carpinteri A. A generalized Paris' law for fatigue crack growth. *J Mech Phys Solids* 2006;**54**(7):1333–49.
- Sun Z, Huang M. Fatigue crack propagation of new aluminum lithium alloy bonded with titanium alloy strap. *Chin J Aeronaut* 2013;**26**(3):601–5.
- Van Horenbeek A, Pintelon L. A dynamic predictive maintenance policy for complex multi-component systems. *Reliab Eng Syst Saf* 2013;**120**:39–50.
- Traore M, Chammas A, Duviella E. Supervision and prognosis architecture based on dynamical classification method for the predictive maintenance of dynamical evolving systems. *Reliab Eng Syst Saf* 2015;**136**:120–31.
- Nguyen K-A, Do P, Grall A. Multi-level predictive maintenance for multi-component systems. *Reliab Eng Syst Saf* 2015;**144**:83–94.
- Curcurù G, Galante G, Lombardo A. A predictive maintenance policy with imperfect monitoring. *Reliab Eng Syst Saf* 2010;**95**(9):989–97.
- Langeron Y, Grall A, Barros A. A modeling framework for deteriorating control system and predictive maintenance of actuators. *Reliab Eng Syst Saf* 2015;**140**:22–36.
- Liu J, Zhang M, Zuo H, Xie J. Remaining useful life prognostics for aeroengine based on superstatistics and information fusion. *Chin J Aeronaut* 2014;**27**(5):1086–96.
- Hu C, Zhou Z, Zhang J, Si X. A survey on life prediction of equipment. *Chin J Aeronaut* 2015;**28**(1):25–33.
- Wang H, Xu T, Mi Q. Lifetime prediction based on Gamma processes from accelerated degradation data. *Chin J Aeronaut* 2015;**28**(1):172–9.
- Wang X, Lin S, Wang S, He Z, Zhang C. Remaining useful life prediction based on the Wiener process for an aviation axial piston pump. *Chin J Aeronaut* 2016;**29**(3):779–88.
- Gebraeel NZ, Lawley MA, Li R, Ryan JK. Residual-life distributions from component degradation signals: A Bayesian approach. *IIE Trans* 2005;**37**(6):543–57.
- Compare M, Zio E. Predictive maintenance by risk sensitive particle filtering. *IEEE Trans Reliab* 2014;**63**(1):134–43.
- Hu Y, Baraldi P, Di Maio F, Zio E. A particle filtering and kernel smoothing-based approach for new design component prognostics. *Reliab Eng Syst Saf* 2015;**134**:19–31.
- Wang W, Carr M. A stochastic filtering based data driven approach for residual life prediction and condition based maintenance decision making support. *Proceedings of the 2010 prog-*

- agnostics and system health management conference; 2010 12–14 Jan. 2010; 2010. p. 1–10.
23. Muheng W, Maoyin C, Zhou D, Wang W. Remaining useful life prediction using a stochastic filtering model with multi-sensor information fusion. *Proceedings of the 2011 prognostics and system health management conference*; 2011 May 24–25; Shenzhen China; 2011. p. 1–6.
 24. Wang Y, Gogu C, Binaud N, Bes C. Predicting remaining useful life by fusing SHM data based on Extended Kalman Filter. *Proceedings of the 25th European safety and reliability conference*; 2015 September 7–10; Zurich, Switzerland; 2015. p. 2489–96.
 25. Lu S, Tu Y-C, Lu H. Predictive condition-based maintenance for continuously deteriorating systems. *Qual Reliab Eng Int* 2007;**23**(1):71–81.
 26. Fink O, Zio E, Weidmann U. A classification framework for predicting components' remaining useful life based on discrete-event diagnostic data. *IEEE Trans Reliab* 2015;**64**(3):1049–56.
 27. Gorguluarslan RM, Choi S-K. Predicting reliability of structural systems using classification method. *Proceedings of the ASME 2013 international design engineering technical conferences and computers and information in engineering conference*; 2013 August 4–7; Portland, USA; 2013. p. V02AT02A030.
 28. Loutas TH, Roulias D, Georgoulas G. Remaining useful life estimation in rolling bearings utilizing data-driven probabilistic E-support vectors regression. *IEEE Trans Reliab* 2013;**62**(4):821–32.
 29. Si XS. An adaptive prognostic approach via nonlinear degradation modeling: application to battery data. *IEEE Trans Ind Electron* 2015;**62**(8):5082–96.
 30. Si XS, Wang W, Hu CH, Zhou DH. Estimating remaining useful life with three-source variability in degradation modeling. *IEEE Trans Reliab* 2014;**63**(1):167–90.
 31. Wang ZQ, Wang W, Hu CH, Si XS, Zhang W. A prognostic-information-based order-replacement policy for a non-repairable critical system in service. *IEEE Trans Reliab* 2015;**64**(2):721–35.
 32. Jardine AKS, Lin D, Banjevic D. A review on machinery diagnostics and prognostics implementing condition-based maintenance. *Mech Syst Signal Proc* 2006;**20**(7):1483–510.
 33. Pattabhiraman S, Gogu C, Kim NH, Haftka RT, Bes C. Skipping unnecessary structural airframe maintenance using an on-board structural health monitoring system. *Proc Inst Mech Eng Part O-J Risk Reliab* 2012;**226**(5):549–60.
 34. Huang B, Du X. Probabilistic uncertainty analysis by mean-value first order Saddlepoint approximation. *Reliab Eng Syst Saf* 2008;**93**(2):325–36.
 35. Grewal MS, Andrews AP. *Kalman filtering: Theory and practice with MATLAB*. Piscataway, NJ: John Wiley & Sons; 2014.
 36. Cortie MB, Garrett GG. On the correlation between the C and m in the Paris equation for fatigue crack propagation. *Eng Fract Mech* 1988;**30**(1):49–58.
 37. Benson JP, Edmonds DV. The relationship between the parameters C and m of Paris' law for fatigue crack growth in a low-alloy steel. *Scripta Mater Scripta Metallurgica* 1978;**12**(7):645–7.
 38. Bilir ÖG. The relationship between the parameters C and n of Paris' law for fatigue crack growth in a SAE 1010 steel. *Eng Fract Mech* 1990;**36**(2):361–4.